Journal of Mahani Mathematical Research

Shahid Bahonar University of Kerman

Print ISSN: 2251-7952 Online ISSN: 2645-4505

THE DESIGN OF GENERALIZED LIKELIHOOD RATIO CONTROL CHART FOR MONITORING THE VON MISES DISTRIBUTED DATA

A.A. KazemiNia, B. Sadeghpour Gildeh, and Z. Abbasi Ganji ✉

Article type: Research Article

(Received: 05 March 2022, Received in revised form: 20 April 2022)

(Accepted: 02 May 2022, Published Online: 05 May 2022)

Abstract. In this paper, a new generalized likelihood ratio (GLR) control chart based on sequentially probability ratio test (SPRT) is introduced to monitor the directional mean of von Mises distribution. Different window size of past samples are utilized to construct the GLR chart statistic, and the performance of this chart in detecting a wide range of parameter shift is evaluated. A simulation study is carried out to investigate the performance of the proposed control chart in comparison with cumulative sum (CUSUM) control chart. To guide practitioners, a real example is provided.

Keywords: : Von Mises distribution, Average run length, SPRT, Maximum likelihood estimation, CUSUM, Generalized likelihood ratio.
2020 MSC: 62A86.

1. Introduction

Von Mises (circular normal) distribution is the most common circular distribution for modeling circular or angular data. As mentioned in [19], directional data are applicable in many fields such as biology, geography, geology, geophysics, medicine, oceanography and meteorology. For example, a biologist may be measuring the direction of flight of a bird, while a meteorologist may be interested in wind directions in a specific region. A set of such observations on directions is said to as directional data.

Suppose X has von Mises distribution, denoted by $vM(\mu, k)$. Its density function has the following form:

$$f(x;\mu,k) = \frac{1}{2\pi I_0(k)} e^{k\cos(x-\mu)}, \quad 0 \leq x < 2\pi, \quad 0 \leq \mu < 2\pi, \quad k \geq 0, \tag{1}$$

where, $I_0(k)$ is the imaginary Bessel function of the first kind, obtained by

$$I_0(k) = \frac{1}{2\pi}\int_0^{2\pi} e^{k\cos(x)}dx = \sum_{i=0}^{\infty}(\frac{k}{2})^{2i}(\frac{1}{i!})^2. \tag{2}$$

✉ abbasiganji@mail.um.ac.ir, ORCID: 0000-0003-1939-0080
DOI: 10.22103/jmmrc.2022.19133.1213
Publisher: Shahid Bahonar University of Kerman
How to cite: A. A. KazemiNia, B. Sadeghpour Gildeh, Z. Abbasi Ganji, *The Design of Generalized Likelihood Ratio Control Chart for Monitoring the von Mises Distributed Data*, J. Mahani Math. Res. 2023; 12(1): 1-13.

The parameter k measures the concentration of the circle normal distribution, and $\frac{1}{k}$ is analogous to σ^2 in the normal distribution in linear case. If $k = 0$, then $vM(\mu, k)$ is circular uniform distribution, and when k is small, the distribution is close to uniform. In fact, as k increases the distribution approaches a normal distribution with mean μ and variance $1/k$. For large value of k, the distribution $vM(\mu, k)$ becomes very concentrated about μ.

Fisher [5], Gadsden and Kanji [6], Laha and Gupta [12], Lombard [15], Mardia [16,17], and Sengupta and Laha [20] worked on the circular distribution and statistical analysis of angular data. In order to apply the sequentially probability ratio test (SPRT) for testing the hypothesis $H_0 : \mu = \mu_0$ versus $H_1 : \mu = \mu_1$, that $\mu_1 \neq \mu_0$. Suppose a random sample of size n as $X_1, X_2, ..., X_n$, with values $x_1, x_2, ..., x_n$ is taken sequentially from a $vM(\mu, k)$, which $K > 0$, so the likelihood function is as the following;

$$L(\mu_1, k, x_1, x_2, ..., x_n) = (\frac{1}{2\pi I_0(k)})^n e^{k \sum_{i=1}^{n} \cos(x_i - \mu_1)}. \tag{3}$$

Then, the log-likelihood function is as:

$$l(\mu_1, k, x_1, x_2, ..., x_n) = -n \log 2\pi + k \sum_{i=1}^{n} \cos(x_i - \mu_1) - n \log I_0(k). \tag{4}$$

Set $\bar{C} = 1/n \sum_{i=1}^{n} \cos(x_i - \mu_1)$, $\bar{S} = 1/n \sum_{i=1}^{n} \sin(x_i - \mu_1)$, and $\bar{R} = \sqrt{\bar{C}^2 + \bar{S}^2}$, so

$$l(\mu_1, k, x_1, x_2, ..., x_n) = n\{-\log 2\pi + k\bar{R} \cos(\bar{x} - \mu_1) - \log I_0(k)\}. \tag{5}$$

Let the concentration parameter is known or constant, then the maximum value of $\cos(x)$ occurs at $x = 0$. Therefore, the maximum likelihood estimate of μ_1 is obtained as what follows;

$$\widehat{\mu}_1 = \bar{x} = \begin{cases} \tan^{-1}(\frac{\bar{S}}{\bar{C}}); & \bar{C} > 0,\ \bar{S} \geq 0, \\ \tan^{-1}(\frac{\bar{S}}{\bar{C}}) + 2\pi; & \bar{C} \geq 0,\ \bar{S} < 0, \\ \tan^{-1}(\frac{\bar{S}}{\bar{C}}) + \pi; & \bar{C} < 0. \end{cases} \tag{6}$$

The maximum likelihood ratio is obtained as:

$$
\begin{aligned}
l_n = \log \frac{L(\mu_1, k, x_1, x_2, ..., x_n)}{L(\mu_0, k, x_1, x_2, ..., x_n)} &= l(\mu_1, k, x_1, x_2, ..., x_n) - l(\mu_0, k, x_1, x_2, ..., x_n) \\
&= k \sum_{i=1}^{n} \big\{ \cos(x_i - \mu_1) - \cos(x_i - \mu_0) \big\} \\
&= 2k \sum_{i=1}^{n} \sin\big(x_i - \frac{\mu_1 + \mu_0}{2}\big) \sin\big(\frac{\mu_1 - \mu_0}{2}\big) \\
&= \sum_{i=1}^{n} Z_i. \qquad (7)
\end{aligned}
$$

Let α and β are type I and II errors of hypothesis testing, respectively, and $A = (1-\beta)/\alpha$, and $B = \beta/(1-\alpha)$. Then, based on the critical values lnA and lnB, there is a three decision problem as what follows;

- If $\sum_{i=1}^{n} Z_i \leq lnB$, then one cannot reject the null hypothesis H_0.
- If $\sum_{i=1}^{n} Z_i \geq lnA$, then the null hypothesis H_0 will be rejected.
- If $lnA < \sum_{i=1}^{n} Z_i < lnB$, then one cannot come to a clear decision and may take an additional sample and follow the procedure until making a decision.

Now, suppose that the concentration parameter is unknown. The maximum likelihood estimation of k_1 is obtained as:

$$\widehat{k}_1 = B^{-1}(\bar{R}), \qquad (8)$$

where $B(k) = I_1(k)/I_0(k)$, and $I_1(k) = 1/2\pi \int_0^{2\pi} \cos(x) e^{k\cos(x)} dx$. Best and Fisher [3] obtained an approximation of $\widehat{k}_1$ as:

$$
\widehat{k}_1 \cong \begin{cases}
2\bar{R} + \bar{R}^3 + \frac{5}{6}\bar{R}^5; & \bar{R} < 0.53, \\
-0.4 + 1.39\bar{R} + \frac{0.43}{1-\bar{R}}; & 0.53 \leq \bar{R} \leq 0.85, \\
\frac{1}{\bar{R}^3 - 4\bar{R}^2 + 3\bar{R}}; & \bar{R} > 0.85.
\end{cases} \qquad (9)
$$

Control charts are graphical and powerful tools in statistical quality control (SQC) to monitor the process stability and detect a shift occurred in in-control parameter to out-of-control value. The Generalized likelihood ratio control chart is effective to detect a wide range of parameter shifts. This type of control chart has not received as much attention in statistical quality control application as Shewhart, CUSUM, and EWMA charts, but the preference of the GLR control chart against other charts is estimation of process change point and shift size. In application, unlike another charts, the GLR control chart does not require specifying control chart parameters to design. In the literature, there have been some researches developing the GLR control charts. For more information, one can see the papers by Apley and Shi [2], Capizzi [4], Gombay [7], Han et al. [8], Hawkins and Zamba [10], KazemiNia et al. [11], Lai [13], Lee et al. [14], Reynolds and Lou [18], Seigmund and Venkatraman [21], and Willsky and Jones [22] worked on this subject. Furthermore, Abbasi Ganji and Sadeghpour Gildeh [1] presents some references in this field.

Average run length (ARL) is one of the most popular performance metric for control charts. It is the expected samples number from starting to shift until the first signal for out of control situation. If the process operates in control for some periods of time $(0,t)$ and then, operates out-of-control at time $(t+1,N)$, the steady state ARL (SSARL) is used, and when $t=0$, the initial state ARL (ISARL) is applied. In this study, the ISARL is utilized to evaluate and compare the control charts abilities.

In this paper, the SPRT method is used to construct the GLR control chart for monitoring the variation of directional mean parameter. Also, the ability of the proposed control chart over wide range of shift is evaluated. In addition, the performance of this chart is compared with the CUSUM chart, developed by Hawkins and Lombard [9]. Furthermore, the corresponding control limits with different ISARL for design the GLR chart is proposed.

2. The GLR control chart for monitoring directional mean

Let the data $x_1, x_2, ..., x_N$ from von Mises distribution with μ and constant or estimated concentration parameter k are available. The in-control value of μ is μ_0. Consider the hypothesis that a directional mean shift to some value μ_1 has occurred at time t^* between samples t and $t+1$, which $t<N$, so the likelihood function at N^{th} sample, based on equation (3), is as what follows;

(10)
$$L(\mu_1, k, x_1, x_2, ..., x_N) = (\frac{1}{2\pi I_0(k)})^N e^{k\left\{\sum_{i=1}^{t}\cos(x_i-\mu_0)+\sum_{i=t+1}^{N}\cos(x_i-\mu_1)\right\}}.$$

The maximum likelihood estimation of unknown parameter μ_1 obtains from equation (6) as $\bar{C} = \sum_{i=t+1}^{N}\cos x_i/(N-t)$, and $\bar{S} = \sum_{i=t+1}^{N}\sin x_i/(N-t)$. When there has been no directional mean shift, the likelihood function at sample N defined as

(11)
$$L(\mu_0, k, x_1, x_2, ..., x_N) = (\frac{1}{2\pi I_0(k)})^N e^{k\sum_{i=1}^{N}\cos(x_i-\mu_0)}.$$

Hence, the GLR control chart statistic is as:

(12)
$$\begin{aligned} R_N &= ln\frac{\max_{0<t\leq N,\ 0<\mu_1<2\pi} L(\mu_1, k, x_1, x_2, ..., x_N)}{L(\mu_0, k, x_1, x_2, ..., x_N)} \\ &= \max_{0<t\leq N} k\sum_{i=t+1}^{N}\cos(x_i-\widehat{\mu}_{1,t}) - \cos(x_i-\mu_0). \end{aligned}$$

Assume $g(t) = k\sum_{i=t+1}^{N}\cos(x_i-\widehat{\mu}_{1,t}) - \cos(x_i-\mu_0)$, so by utilizing the window size m of past samples, the chart statistic has the form

$$R_{N,m} = \begin{cases} \max_{0<t\leq N} g(t); & N \leq m, \\ \max_{N-m<t\leq N} g(t); & N > m. \end{cases} \tag{13}$$

The control chart signals if $R_{N,m} > h_{GLR}$, where h_{GLR} is a predetermined control limit chosen to achieve the desired ISARL from an in-control process.

Simulation schemes with 5000 iterations and total sample number $N = 10000$ is applied to search the best window size and control chart limit. The values of ISARL for different window sizes are presented in Table 1 to demonstrate the effect of window size on the sensitivity of the control chart in detecting process shift, similar to the approach discussed in Reynolds and Lou [18].

Table 1. The ISARL values of the GLR control chart for $k = 3$, and different values of window

	m										
	1	10	20	35	50	100	200	300	400	900	1000
shift size	[1]	[2]	[3]	[4]	[5]	[6]	[7]	[8]	[9]	[10]	[11]
0	**369.959**	369.959	369.959	369.959	369.959	369.959	369.959	369.959	**369.959**	369.959	369.959
0.039	**360.453**	300.322	200.112	77.581	54.634	27.618	25.604	23.031	**22.104**	22.698	24.137
0.052	**306.342**	201.116	121.054	61.523	43.401	23.862	17.594	15.736	**10.521**	17.103	17.134
0.079	**258.236**	172.315	101.085	47.342	22.141	11.612	7.855	4.442	**4.162**	5.099	6.324
0.105	**203.457**	155.324	81.403	30.519	12.762	6.103	3.445	1.832	**1.832**	2.678	3.008
0.157	**188.231**	121.584	69.545	19.108	5.326	2.327	1.901	1.031	**1.014**	1.931	2.011
0.314	**58.206**	44.938	22.347	6.693	3.412	1.734	1.192	0.872	**0.612**	0.967	1.523
0.393	**30.162**	20.431	10.319	3.087	1.321	1.145	0.622	0.544	**0.544**	0.675	0.675
0.785	**5.323**	4.602	3.091	1.034	0.819	0.736	0.545	0.515	**0.513**	0.55	0.55
1.047	**1.013**	1.004	1.003	0.723	0.711	0.674	0.525	0.507	**0.507**	0.51	0.51
1.571	**0.501**	0.505	0.505	0.505	0.505	0.505	0.505	0.503	**0.503**	0.505	0.505
h_{GLR}	4.982	5.423	5.657	5.712	5.745	5.789	6.231	6.443	6.612	6.653	6.773

Assume that the size of shift in directional mean is $\mu - \mu_0$, whereas $\mu > \mu_0$. The control chart limits were adjusted to reach an in-control ARL for 370 ($ARL_0 = 370$). From Table 1, it is found that the GLR control chart with $m = 1$, has less sensitive performance in detecting the small shifts, while is sensitive for detecting large shifts. Increasing the window size improves the ability of this control chart in detecting the small and intermediate shifts. On the other hand, selecting large value of window size is equivalent to the control chart without window size. It can be seen that $m = 400$ is the best window size for the GLR control chart to detect parameter shifts.

Control limits h_{GLR} of the GLR control chart corresponds to some specified in-control ARL are presented in Table 2. To find h_{GLR}, the linear interpolation method is used.

TABLE 2. The control limit of GLR control chart according to in control ARL and $m = 400$

	k							
	0.1	0.5	1	2	3	4	5	6
ICARL	[1]	[1]	[1]	[2]	[3]	[4]	[5]	[6]
100	3.102	4.826	5.321	5.774	6.237	6.425	6.565	6.872
200	4.011	5.225	5.645	6.104	6.348	6.661	6.684	6.935
300	4.324	5.786	6.327	6.448	6.569	6.709	6.723	6.967
370	5.028	6.127	6.553	6.572	6.621	6.746	6.763	7.203
450	5.412	6.326	6.647	6.675	6.691	6.941	7.132	7.357
550	5.625	6.537	6.708	6.751	6.852	7.205	7.462	7.683
800	5.814	7.219	7.472	7.601	7.853	7.972	8.405	8.749

3. The CUSUM chart for monitoring directional mean

As mentioned in the paper by Hawkins and Lombard [9], when the concentration parameter k remains fixed and directional mean parameter μ may change from its in-control value μ_0 to some out of control value μ_1, the CUSUM chart statistic for detecting the occurred shift defined as

$$C_N = max\{0, C_{N-1} + k\big[\cos(x_N - \mu_1) - \cos(x_N - \mu_0)\big]\}, \quad (14)$$

or

$$C_N = max\{0, C_{N-1} + 2k\sin(x_N - \frac{\mu_1 + \mu_0}{2})\sin(\frac{\mu_1 - \mu_0}{2})\}. \quad (15)$$

The CUSUM chart statistic signals at sample N, when $C_N > h_C$, where h_C is the upper control limit selected according to a specified in-control ARL.

To design the CUSUM chart, the value of μ_1 must be specified as a tuning parameter, even though the actual value of the shift is unknown. Table 3 presents the ISARL values of the CUSUM chart with some tuning parameters (such as $\mu_1 = \pi/80 = 0.039$) to illustrate the performance of this chart for detecting the parameter shifts. This table gives the control chart limit adjusted to achieve an in-control ARL of 370.

From Table 3, it can be concluded that selecting the tuning parameter near to the actual shift improves the ability of the CUSUM chart in detecting parameter shift. For example, the best tuning parameter value to detect the occurred shift size 1.57, is $\mu_1 = \pi/2 = 1.57$, and some of this type cases are bolded in Table 3. Increasing the value of tuning parameter, decreases the ability of the chart in detecting the small shifts, and increases its ability in detecting the intermediate and large shifts.

TABLE 3. ISARL values of the CUSUM chart for $k = 3$, and some tuning parameter values

	μ_1				
	0.039	0.105	0.314	0.785	1.571
shift size	[1]	[2]	[3]	[4]	[5]
0	369.959	369.959	369.959	369.959	369.959
0.039	**21.692**	27.452	89.84	2 222.416	295.096
0.052	10.701	12.365	62.807	187.329	282.465
0.079	3.924	4.232	22.735	118.392	225.489
0.105	1.945	**1.868**	8.564	81.784	196.894
0.157	1.139	1.01	1.984	38.097	142.052
0.314	0.718	0.65	**0.592**	3.164	45.471
0.393	0.668	0.614	0.561	0.893	25.019
0.785	0.581	0.554	0.523	**0.514**	0.708
1.047	0.565	0.542	0.517	0.508	0.511
1.571	0.555	0.535	0.513	0.505	**0.504**
h_C	2.857	4.98	5.756	5.475	5.104

The best performance of the CUSUM chart is achieved when the tuning parameter is equal to actual shift. In fact, this is disadvantage of the CUSUM chart, because in practice area, the real shift is unknown. Based on the tables 1 and 3, the CUSUM chart with special tuning parameter (equal or next to the shift size) in some cases has a better performance against the GLR control chart, but the overall performance of the GLR control chart with $m = 400$ is better than the CUSUM chart. In addition, despite the CUSUM chart, the advantage of the GLR control chart is detecting the unknown shift without determining the tuning parameter.

4. An application to real data

In the application, the proposed control chart can be used for monitoring circular distributed data that arise whenever directions are measured, and usually expressed as angles, such as monitoring the transporting matter data from one place to another in time (geological processes), wind speed and directions data (meteorological processes), bird orientation data in homing and migration (biological processes), the occurrence of earthquakes data in a region, the longitude and latitude of each shock (geographical processes), a periodic phenomenon data with known period (economical processes), sound waves or molecular links data, experiments results on divers and swimmers under water to simulate zero-gravity in space travel (physical processes), circadian rhythm data of systolic blood pressure, and the number of deaths due to a disease or the number of onsets of a disease in each month over years (medical processes), and monitoring the airway of airplanes and rockets and astronomical processes.

Monitoring the wind speed and direction are important for predicting weather patterns and global climate. Wind speed and direction have numerous impacts on surface water. These parameters affect rates of evaporation, mixing of surface waters, and the development of seiches and storm surges. Each of these processes has dramatic effects on water quality and water level.

Wind direction is an instance of circular data that can vary over 360°, and can be represented as a point on a unit circle. Tables 4 and 5, and also Figure 1 present the wind direction taken hourly at Mesa Verde National Park (U.S National Park Service, Air Resources Division, from 07/05/2018 to 07/12/2018-https://www.nps.gov/subjects/air/current-data.htm?site=meve).

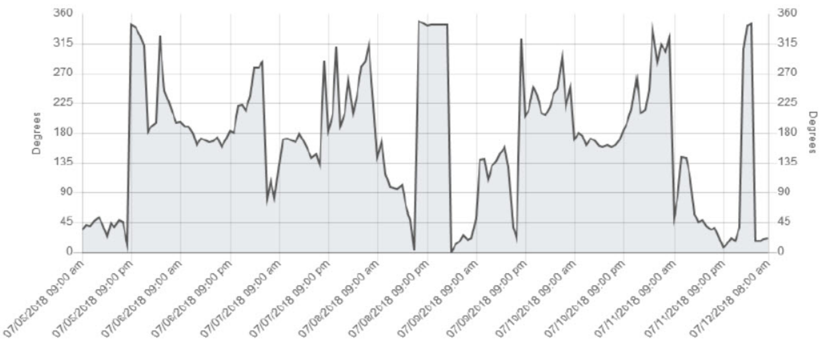

Figure 1. Wind direction taken hourly at Mesa Verde National Park (U.S National Park Service, Air Resources Division, from 07/05/2018 to 07/12/2018)

The proposed GLR control chart is utilized to monitor wind direction data (with radian transformation). The in-control directional mean and concentration parameter are estimated as 2.786 and 0.221, respectively. The window size ($m = 400$) and control limit $h_{GLR} = 6.1$ are considered corresponding to in-control ARL 370. Based on the Figure 2, the GLR control chart signals the out-of-control wind direction at Thursday, July 12^{th}. An estimation of directional mean of this day is obtained as 0.109.

TABLE 4. Wind direction taken hourly at Mesa Verde National Park (U.S National Park Service, Air Resources Division, from 07/05/2018 to 07/08/2018)

Thursday, July 5^{th}		Friday, July 6^{th}		Saturday, July 7^{th}		Sunday, July 8^{th}	
time	degree	time	degree	time	degree	time	degree
11:00 PM	330	12:00 AM	221	11:00 PM	311	11:00 PM	343
10:00 PM	339	10:00 PM	180	10:00 PM	208	10:00 PM	343
9:00 PM	343	9:00 PM	183	9:00 PM	183	9:00 PM	342
8:00 PM	12	8:00 PM	169	8:00 PM	290	8:00 PM	346
7:00 PM	45	7:00 PM	158	7:00 PM	131	7:00 PM	349
6:00 PM	48	6:00 PM	172	6:00 PM	147	6:00 PM	3
5:00 PM	39	5:00 PM	167	5:00 PM	142	5:00 PM	49
4:00 PM	44	4:00 PM	165	4:00 PM	154	4:00 PM	70
3:00 PM	24	3:00 PM	169	3:00 PM	168	3:00 PM	101
2:00 PM	43	2:00 PM	171	2:00 PM	178	2:00 PM	95
1:00 PM	53	1:00 PM	162	1:00 PM	165	1:00 PM	96
12:00 PM	47	12:00 PM	179	12:00 PM	169	12:00 PM	98
11:00 AM	40	11:00 AM	190	11:00 AM	171	11:00 AM	118
10:00 AM	42	10:00 AM	189	10:00 AM	170	10:00 AM	168
9:00 AM	34	9:00 AM	197	9:00 AM	132	9:00 AM	143
		8:00 AM	195	8:00 AM	81	8:00 AM	222
		7:00 AM	209	7:00 AM	108	7:00 AM	314
		6:00 AM	229	6:00 AM	80	6:00 AM	287
		5:00 AM	244	5:00 AM	287	5:00 AM	280
		4:00 AM	326	4:00 AM	279	4:00 AM	236
		3:00 AM	195	3:00 AM	279	3:00 AM	209
		2:00 AM	189	2:00 AM	236	2:00 AM	259
		1:00 AM	181	1:00 AM	213	1:00 AM	210
		12:00 AM	313	12:00 AM	222	12:00 AM	190

Table 5. Wind direction taken hourly at Mesa Verde National Park (U.S National Park Service, Air Resources Division, from 07/09/2018 to 07/12/2018)

Monday, July 9^{th}		Tuesday, July 10^{th}		Wednesday, July 11^{th}		Thursday, July 12^{th}	
time	degree	time	degree	time	degree	time	degree
12:00 AM	249	11:00 PM	216	11:00 PM	21	8:00 AM	22
10:00 PM	215	10:00 PM	198	10:00 PM	11	7:00 AM	20
9:00 PM	205	9:00 PM	183	9:00 PM	7	6:00 AM	17
8:00 PM	322	8:00 PM	169	8:00 PM	25	5:00 AM	18
7:00 PM	20	7:00 PM	161	7:00 PM	37	4:00 AM	345
6:00 PM	38	6:00 PM	158	6:00 PM	34	3:00 AM	342
5:00 PM	127	5:00 PM	162	5:00 PM	40	2:00 AM	307
4:00 PM	159	4:00 PM	158	4:00 PM	49	1:00 AM	38
3:00 PM	148	3:00 PM	160	3:00 PM	45	12:00 AM	18
2:00 PM	137	2:00 PM	169	2:00 PM	58		
1:00 PM	129	1:00 PM	171	1:00 PM	116		
12:00 PM	109	12:00 PM	162	12:00 PM	141		
11:00 AM	140	11:00 AM	176	11:00 AM	143		
10:00 AM	139	10:00 AM	180	10:00 AM	84		
9:00 AM	51	9:00 AM	170	9:00 AM	52		
8:00 AM	22	8:00 AM	249	8:00 AM	324		
7:00 AM	19	7:00 AM	220	7:00 AM	302		
6:00 AM	26	6:00 AM	294	6:00 AM	314		
5:00 AM	16	5:00 AM	246	5:00 AM	287		
4:00 AM	12	4:00 AM	239	4:00 AM	337		
3:00 AM	0	3:00 AM	220	3:00 AM	245		
2:00 AM	344	2:00 AM	207	2:00 AM	215		
1:00 AM	343	1:00 AM	209	1:00 AM	210		
12:00 AM	343	12:00 AM	236	12:00 AM	260		

5. Conclusion

In this paper, the design of the GLR control chart for monitoring the directional mean parameter shifts in von Mises distributed process is studied,

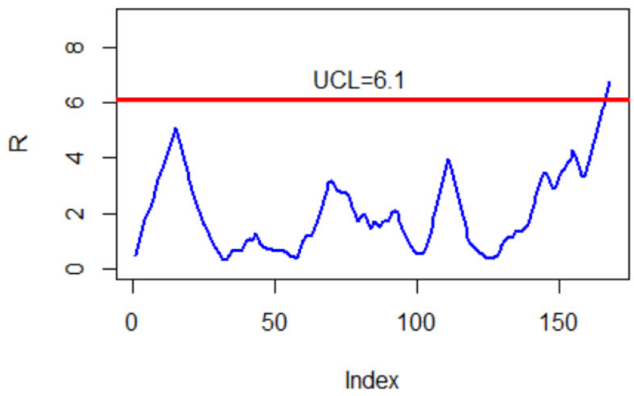

FIGURE 2. The GLR chart of wind direction with $m = 400$, $\mu_0 = 2.786$, $k = 0.221$, and $h_{GLR} = 6.1$

and the performance of the proposed chart is evaluated in view of Monte Carlo simulations. Furthermore, the performance of the GLR control chart with the CUSUM chart is compared based on ARL criterion. It is concluded that the GLR control chart has better and more accurate performance than the CUSUM chart in detecting parameter shifts. The determination of the control limit and window size in the GLR control chart is conducted based on simulations. Finally, the proposed control chart is used to monitor the directional mean parameter shifts in wind direction process.

6. Aknowledgement

We would like to thank the reviewers for their thoughtful comments and efforts towards improving our manuscript.

References

[1] Abbasi Ganji Z, Sadeghpour Gildeh B (2022) A likelihood control chart for monitoring bivariate lifetime processes. Journal of Mahani Mathematical Research center, 11 (2): 97-118.
[2] Apley DW, & Shi J (1999) The GLRT for statistical process control of auto correlated processes. IIE Transactions, 31 (12): 1123-1134.
[3] Best DJ, and Fisher NI (1981) The BIAS of the maximum likelihood estimators of the von Mises-Fisher concentration parameters: the BIAS of the maximum likelihood estimators. Communications in Statistics-Simulation and Computation, 10 (5): 493-502.
[4] Capizzi G (2001) Design of change detection algorithms based on the generalized likelihood ratio test. Environ metrics: The official journal of the International Environ metrics Society, 12 (8): 749-756.
[5] Fisher NI (1995) Statistical analysis of circular data. Cambridge University Press.
[6] Gadsden RJ, and Kanji GK (1981) Sequential analysis for angular data. The Statistician, 119-129.

[7] Gombay E (2000) Sequential change-point detection with likelihood ratios. Statistics & probability letters, 49 (2): 195-204.
[8] Han D, Tsung F, Hu X, and Wang, K (2007) CUSUM and EWMA multi-charts for detecting a range of mean shifts. Statistica Sinica, 17 (3): 1139-1164.
[9] Hawkins DM, and Lombard F (2017) Cusum control for data following the von Mises distribution.Journal of Applied Statistics, 44 (8): 1319-1332.
[10] Hawkins DM, and Zamba KD (2005) Statistical process control for shifts in mean or variance using a change point formulation. Technimetrics, 47 (2): 164-173.
[11] KazemiNia A, Sadeghpour Gildeh B, and Abbasi Ganji Z (2018) The design of geometric generalized likelihood ratio control chart. Quality and Reliability Engineering International, 34 (5): 953-965.
[12] Laha AK, Gupta A (2011) Statistical Quality Control of Directional Data 2nd IIMA International Conference on Advanced Data Analysis, Business Analytics and Intelligence, Ahmedabad.
[13] Lai TL (1995) Sequential change point detection in quality control and dynamical systems. Journal of the Royal Statistical Society Series B (Methodological), 57 (4): 613-658.
[14] Lee J, Peng Y, Wang N, and Reynolds MR (2017) A GLR control chart for monitoring a multinomial process. Quality and Reliability Engineering, 33 (8): 1773-1782.
[15] Lombard F (1986) The change–point problem for angular data: a nonparametric approach. Technometrics, 28 (4): 391-397.
[16] Mardia KV (1975) Statistics of directional data. Journal of the Royal Statistical Society. Series B (Methodological), 37 (3): 349-393.
[17] Mardia KV, Jupp PE (2009) Directional statistics. John Wiley & Sons, vol. 494.
[18] Reynolds Jr. MR, and Lou J (2010) An evaluation of a GLR control chart for monitoring the process mean. Journal of quality technology, 42 (3): 287-310.
[19] Peker KÖ, Bacanli S (2007) a sequential test for the mean direction applied to circular data and an application. Eskisehir Osmangazi Üniversitesi Müh.Mim.Fak.Dergisi, C.XX, S.2.
[20] Sengupta A, and Laha AK (2008) A Bayesian analysis of the change-point problem for directional data. Journal of Applied Statistics, 35 (6): 693-700.
[21] Siegmund D, and Venkatraman ES (1995) Using the generalized likelihood ratio statistic for sequential detection of a change-point. The Annals of Statistics, 23 (1): 255-271.
[22] Willsky A, Jones H (1976) A generalized likelihood ratio approach to the detection and estimation of jumps in linear systems. IEEE Transactions on Automatic control, 21 (1): 108-112.

Ali Akbar KazemiNia
Orcid number: 0000-0001-8371-118X
Department of Statistics
Faculty of Mathematical Sciences
Ferdowsi University of Mashhad
Mashhad, Iran
Email address: um.kazeminia@gmail.com

Bahram Sadeghpour Gildeh
Orcid number: 0000-0003-0863-676X
Department of Statistics
Faculty of Mathematical Sciences
Ferdowsi University of Mashhad
Mashhad, Iran
Email address: sadeghpour@um.ac.ir

Zainab Abbasi Ganji
Orcid number: 0000-0003-1939-0080
Khorasan Razavi Agricultural and Natural Resources Research and Education Center, AREEO
Mashhad, Iran
Email address: z.ganji@areeo.ac.ir, abbasiganji@mail.um.ac.ir